

## MODE-SWITCHING TIMESCALES IN THE CLASSICAL VARIABLE STARS

J. ROBERT BUCHLER<sup>1</sup> AND ZOLTÁN KOLLÁTH<sup>2</sup>

Received 2001 October 22; accepted 2002 March 7

### ABSTRACT

Near the edges of the instability strip, the rate of stellar evolution is larger than the growth rate of the pulsation amplitude, and the same holds whenever the star is engaged in pulsational mode switching. Stellar evolution therefore controls the onset of pulsation at the edges of the instability strip and of mode switching inside it. Two types of switchings (bifurcations) occur. In a soft bifurcation, the switching timescale is the inverse harmonic mean of the pulsational modal growth rate and of the stellar evolution rate. In a hard bifurcation, the switching times can be substantially longer than the thermal timescale, which is typically of the order of 100 periods for Cepheids and RR Lyrae stars. We discuss some of the observational consequences, in particular the paucity of low-amplitude pulsators at the edges of the instability strip.

*Subject headings:* Cepheids — instabilities — stars: evolution — stars: oscillations — stars: variables: other

### 1. INTRODUCTION

The Cepheid and RR Lyrae instability strips (ISs) are observed to be rich in behavior, as seen, for example, in the beautiful work of Udalski et al. (1999), with stars undergoing single-mode (SM) pulsations in the fundamental (F) mode, in the first (O1) or second (O2) overtone, or beat pulsations in two modes (also called double-mode [DM] pulsations). Theoretical work has shown that for the Galactic Cepheids, we have a good understanding of the F and O1 Cepheids (Moskalik, Buchler, & Marom 1992; Bono, Marconi, & Stellingwerf 2000; Feuchtinger, Buchler, & Kolláth 2000) and of RR Lyrae (Feuchtinger 1999). Furthermore, the problem of DM Cepheids and RR Lyrae stars has finally been solved (Kolláth et al. 1998; Feuchtinger 1998, Kolláth et al. 2002, hereafter KBSC02; Kolláth & Buchler 2001, hereafter KB01). However, some small problems remain in RR Lyrae (Kolláth, Buchler, & Feuchtinger 2000) and Cepheids, in particular those with low metallicity (e.g., M. Feuchtinger et al. 2002, in preparation).

As the stars navigate through the IS, their structure undergoes changes. Accordingly, the allowed stable pulsational states change on an evolutionary timescale, and the stars need to switch their pulsational behavior. During some stages, more than one type of pulsational behavior is possible. Some of these pulsational states may be reachable, while other may not be (because a finite-amplitude kick would be required). Stars can therefore be in a different pulsational state at the same place on the blueward and the redward tracks (hysteresis), as, for example, in the case of Cepheids and RR Lyrae. Some classical Cepheids and RR Lyrae stars have been observed to change their pulsational status on human timescales. For example, the pulsation amplitude of Polaris has decreased dramatically over several decades (e.g., Kamper & Fernie 1998). Changes have also occurred in RR Lyrae variables (e.g., Clement & Goranskij 1999). The theoretical aspects of these mode switchings have been addressed in the past (e.g., Stellingwerf 1975; Bono, Castellani, & Stellingwerf 1995), but many of the

questions that observations pose have remained unanswered. For example, observations indicate a paucity of low-amplitude s-Cepheids and fundamental Cepheids (e.g., Fernie et al. 1995 for the Galaxy;<sup>3</sup> J. P. Beaulieu 2001, private communication, for LMC and SMC) and no stars with low-component amplitudes in the DM region (J. P. Beaulieu 2001, private communication; see Fig. 4 in Buchler 1998). A similar situation occurs for RR Lyrae stars (e.g., Walker & Nemec 1996; Walker 1998; Udalski et al. 1997). These deficiencies of small-amplitude pulsators seem too large to be solely due to observational bias.

Here we address the problem of mode switching in a novel fashion, by taking temporal evolution explicitly into account. Hydrodynamical modeling, to be feasible, has typically decoupled pulsation from evolution (usually called a quasi-static approximation). The decoupling allowed the calculation of all the possible full-amplitude and steady pulsational states of a given model at any point along the evolutionary track, i.e., of a sequence of models. However, this quasi-static approximation can break down near the bifurcation points where the star has to switch from one behavior to another (e.g., Lebovitz 1990). (A bifurcation point is where there occurs a qualitative change in the modal behavior). The reason is that, right at a bifurcation point, the growth rate of a mode or limit cycle can vanish and remain small in the vicinity. This causes a temporal delay for the pulsation to achieve the full amplitude that the hydrodynamical modeling would suggest; *the pulsational behavior is then controlled by evolution*. In this paper, we make use of the amplitude equation formalism (Buchler & Goupil 1984; Buchler 1993), which is perfectly tailored to the study of what is happening in the vicinity of the modal bifurcation points, and we show that there are observational consequences.

### 2. ANALYTICAL CONSIDERATIONS

We are led to distinguish two different types of mode switchings that we label soft and hard. A soft bifurcation

<sup>1</sup> Physics Department, University of Florida, Gainesville, FL 32611; buchler@phys.ufl.edu.

<sup>2</sup> Konkoly Observatory, Budapest, Hungary; kollath@konkoly.hu.

<sup>3</sup> See <http://ddo.astro.utoronto.ca/cepheids.html>.

occurs when the nascent mode starts off with infinitesimal amplitude and the growth rate is also infinitesimal. At a hard bifurcation, the stable fixed point disappears (the current pulsational behavior is no longer allowed), and the star is left looking for another stable fixed point (i.e., another pulsational behavior). The rate of change of the amplitude is generally *not* infinitesimally small in this case. In § 3 we see examples of the two types of switchings.

## 2.1. Soft Bifurcations

### 2.1.1. Hopf Bifurcation

We first consider the simplest soft modal switching that occurs when the star enters or exits the IS. Without lack of generality, let us consider the neighborhood of the blue edge, where the linear growth rate  $\kappa$  of a mode, the fundamental or the first or second overtone depending on the luminosity, changes from negative (vibrationally stable) to positive (unstable). Generically, in the vicinity of the blue edge,  $\kappa(t)$  varies proportionately to time,  $\kappa = \chi t$ , where the origin of time is taken to be the passage through the blue edge. The quantity  $\chi = d\kappa/dt$  is therefore the stellar evolutionary rate of change of the linear growth rate. This type of bifurcation is well known to dynamicists and goes under the name of supercritical Hopf bifurcation (e.g., Bergé et al. 1984). The behavior of the amplitude is governed by an amplitude equation of the form (e.g., Buchler & Goupil 1984; Coulet & Spiegel 1984)

$$\frac{d}{dt}A = \kappa(t)A - q(t)A^3 \quad \text{with} \quad \kappa(t) = \chi t, \quad (1)$$

where  $\kappa(t)$  is the instantaneous linear growth rate of the mode, and  $q(t)$  is a nonlinear saturation term that varies little along an evolutionary track.

If the star were perturbed away from its quasi-static stable limit cycle amplitude

$$A_{qs}(t) = \sqrt{\kappa(t)/q(t)}, \quad (2)$$

(as obtained from setting  $dA/dt = 0$  in eq. [1]), it would return to it on a  $t_{th} \sim \kappa^{-1}$  timescale, i.e., over a few hundred pulsations, because the relative growth rates are typically of the order of 1% inside the IS. Away from the bifurcation, the thermal timescale  $t_{th}$  is much shorter than the stellar evolution timescale  $t_{ev} \sim (d \ln T_{eff}/dt)^{-1}$ .

Right at the bifurcation, however,  $\kappa$  vanishes by definition, and it remains small in some neighborhood, so that  $t_{th} \gg t_{ev}$  for a while, and the amplitude does not grow. In fact, the star must wait for evolution to increase the value of  $\kappa$ . Only then can the amplitude catch up with its quasi-static value  $A_{qs}(t)$ . It should be clear from this discussion that *the evolutionary rate of change of the growth rate  $\chi$  will play a crucial role.*

Let us call  $\hat{t}$  the time when the solution catches up and  $\hat{A}$  the amplitude at that instant. We are interested in determining the dependence of  $\hat{t}$  and  $\hat{A} = A_{qs}(\hat{t})$  on  $\chi$ ,  $q$ , and  $A_0 = A(t_0)$ . The latter is the pulsation amplitude at  $t_0$  that arises because of noise in the star.

The coefficient  $q$  is time dependent because of changes in the structure of the star as it evolves, but its time dependence is small. In a later example of an actual RR Lyrae model, we include its time dependence. Here, we approximate  $q$  as a constant. With the substitution  $E = A^2$ , we can then readily

solve equation (1) in the form

$$E(t)^{-1} \simeq e^{-\chi t^2}/E_0 + 2q \int_{t_0}^t e^{-\chi(t'^2 - t^2)} dt' \\ \simeq e^{-\chi t^2}/E_0 + q/(\chi t), \quad (3)$$

where the last expression is the first term of an asymptotic expansion for the integral for large  $\chi t^2$ .

The point at which the pulsation amplitude catches up with the quasi-static value can be obtained to a good approximation by requiring that the first term on the right-hand side of equation (3), which completely dominates at first, becomes a fraction  $\xi$  of the second term ( $\xi = 0.1$  turns out to be a good value). With the help of equation (3), this yields a simple transcendental equation

$$2u - \ln u - \ln f = 0, \quad \text{where} \quad u = \chi t^2, \quad (4)$$

$$\text{and} \quad f = \frac{\chi}{(\xi q A_0^2)^2}. \quad (5)$$

A good approximation to the solution, when  $f$  is large, is obtained with the fitting expression

$$\hat{u} = \chi \hat{t}^2 \sim 1.2 \log f + 0.7. \quad (6)$$

Finally, we have  $\hat{t} = (\hat{u}/\chi)^{1/2}$ . The quantity  $q$  can be re-expressed in terms of the maximum pulsation amplitude in the IS, since  $q A_{\max}^2 = \kappa_{\max}$ . Thus,  $\hat{A}/A_{\max} = (\chi \hat{t}/\kappa_{\max})^{1/2}$ .

The typical behavior of  $A(t)$  as computed from equation (1) is plotted as solid lines in Figure 1 for  $\log \chi = -16$  and for three values of  $A_0$  (from left to right:  $\log E_0 = -14, -16$ , and  $-18$ ). The quantity  $q$ , which scales the amplitude, has been arbitrarily set to  $q = 10^{-6}$ . Shown as a dotted line is the quasi-static limit cycle amplitude  $A_{qs}(t) = (\chi t/q)^{1/2}$ , namely, the value that the amplitude would achieve if the system could react instantly.

We have no knowledge of the intensity of the fluctuation  $A_0$  in a star that represents the projection of the turbulent

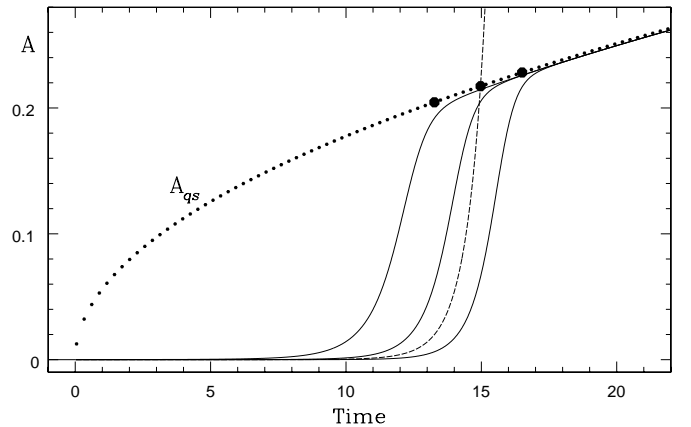


FIG. 1.—Temporal behavior of the pulsation amplitude after the star enters the IS (solid line), for the case of  $\chi = 10^{-16} \text{ s}^{-2}$ . Solid lines are for three values of initial perturbation (noise level)  $\log A_0 = -14, -16$ , and  $-18$ . The dotted line represents the quasi-static amplitude  $A_{qs}(t)$  that would be achieved if the pulsation could react infinitely fast to evolutionary changes in  $\kappa$ . The amplitude scale is set by the choice  $q = 10^{-6}$ . The thick dots correspond to the  $\hat{A}$  obtained with the approximation of eq. (6). The dashed line represents  $A_0 \exp(\frac{1}{2} \chi t^2) / \xi$  for the middle value of  $A_0$ .

noise on the eigenvector of the mode. As suggested by the approximation formula, the larger  $A_0$  is, the faster the amplitude grows (Fig. 1). But note that the effect is only logarithmic, and therefore, a precise knowledge of  $A_0$  is of little importance. *It is the rate of change of the growth rate,  $\chi$ , that sets the switching timescale*, i.e., the scale of the abscissa in Figure 1.

The three larger filled circles in Figure 1 denote the  $\hat{t}$  and  $\hat{A}$  for the three values of  $A_0$  as given by the fitting formula. It can be seen that they provide an excellent agreement with the numerical integrations of equation (1). The dashed line represents  $A_0 \exp(\frac{1}{2} \chi t^2) / \xi$  for the middle value of  $A_0$ .

### 2.1.2. SM to DM Bifurcation

When two (nonresonant) excited modes are involved, equation (1) must be replaced by the two coupled amplitude equations for modes 1 and 2 (e.g., Buchler & Goupil 1984),

$$\dot{A}_1 = [\kappa_1(t) + q_{11}(t)A_1^2 + q_{12}(t)A_2^2 + s_1(t)A_1^2A_2^2]A_1, \quad (7a)$$

$$\dot{A}_2 = [\kappa_2(t) + q_{21}(t)A_1^2 + q_{22}(t)A_2^2 + s_2(t)A_1^2A_2^2]A_2. \quad (7b)$$

We have kept some of the quintic terms in these equations that are necessary in order to describe the observed modal behavior (KB01; KBSC02; earlier studies by Buchler & Kovács [1987] had hoped to get away with retaining only the cubic ones).

When the transition from SM to DM inside the IS is such that the nascent mode starts with infinitesimal amplitude, as we assume in this section on soft bifurcations, then the behavior of this amplitude is very similar to the Hopf bifurcation that we have just described. The reason is easy to see: in the vicinity of the bifurcation, the amplitude of the finite-amplitude mode (say,  $A_1$ ) changes very little, and we can expand around this point, which leads to an equation for the amplitude, say,  $A_2$  of the nascent mode that is identical to equation (1).

To summarize then, stellar evolution causes a delay of the order of  $\chi^{-1/2}$ , during which the pulsation amplitude stays negligibly small, but after which it very rapidly achieves its quasi-static value. The time spent at the small intermediate amplitudes is therefore very small, and the stars are very unlikely to be observed with such small amplitudes. The amplitude at catch-up,  $\hat{A} \sim \chi^{1/4}$ , thus also depends on  $\chi$ , and when the stellar evolution is slow it will be large. Finally, we note that the timescale and the catch-up amplitude are both insensitive to the poorly known noise level, typified by  $A_0$ .

### 2.2. Hard Bifurcations

A hard bifurcation occurs when, as a result of stellar evolution, a fixed point merges with another unstable fixed point in a mutual annihilation. One can readily visualize this in an amplitude-amplitude plane (see, e.g., KB01; KBSC02), where the fixed points, stable and unstable, lie at the intersection of two loci (curves). As  $T_{\text{eff}}$  changes with evolution, the two intersection points coalesce and then disappear as the curves move apart. At that point, the star has no choice but to look for another stable pulsational state to move into. The new type of pulsation depends on the overall topography at the time and is determined by which fixed point attracts the stellar model. One might think that the time to attain the new pulsational state is the thermal timescale  $t_{\text{th}} = \kappa^{-1}$ , but it can be and is generally much longer,

as we show in a realistic example. We note that for a hard bifurcation, the stellar evolution timescale plays no important role, because the amplitude growth rates do not vanish, and thus the timescale for amplitude change is always finite (KBSC02).

## 3. CEPHEIDS AND RR LYRAE

### 3.1. The Blue Edge

Let us consider first a redward-evolving  $6 M_{\odot}$  Cepheid that enters the first overtone IS. We use equation (6) to estimate the minimum observable amplitude  $\hat{A}$ . Stellar evolution calculations indicate that a  $6 M_{\odot}$  Cepheid variable evolves at a rate of  $dT_{\text{eff}}/dt \sim 2 \times 10^{-10} \text{ K s}^{-1}$  when entering the overtone blue edge (e.g., Alibert et al. 1999). Linear models give a rate of change  $d\kappa/dT_{\text{eff}} \sim 2 \times 10^{-10} (\text{K s})^{-1}$ , so that we obtain  $\chi \sim 4 \times 10^{-20} \text{ s}^{-2}$ . The maximum growth rate  $\kappa_{\text{max}}$  in the IS is  $4 \times 10^{-8} \text{ s}^{-1}$ . If we assume intrinsic fluctuations of the order of  $A_0/A_{\text{max}} \sim 10^{-10}$ , where  $A_{\text{max}}$  is the maximum amplitude in the instability strip, we find that the  $\hat{u}$  in equation (6) takes on values around 35–40. Thus, we estimate that  $\hat{A}/A_{\text{max}} \sim 0.1$  at the blue edge, and that the pulsation amplitude stays negligibly small for  $\hat{t} \sim 1000 \text{ yr}$ ; then it increases very rapidly to a value 10% of the maximum amplitude in the IS. Because of this rapid increase of the amplitude, very few overtone Cepheids with amplitudes less than  $\hat{A} \sim A_{\text{max}}$  should be observed near the blue edge.

Turning now to an  $8 M_{\odot}$  Cepheid that evolves at  $dT_{\text{eff}}/dt \sim 2 \times 10^{-9} \text{ K s}^{-1}$  (Alibert et al. 1999) when entering the fundamental blue edge, with a  $d\kappa/dT_{\text{eff}} \sim 4 \times 10^{-11} (\text{K s})^{-1}$  we obtain  $\chi \sim 8 \times 10^{-20} \text{ s}^{-2}$ . The maximum  $\kappa_{\text{max}}$  in the IS is  $\sim 7 \times 10^{-9} \text{ s}^{-1}$ . Thus, we estimate that again  $\hat{A}/A_{\text{max}} \sim 0.1$  near the blue edge and that the pulsation amplitude stays negligibly small for  $\hat{t} \sim 800 \text{ yr}$ .

Cepheids evolve both blueward and redward. Only half of the Cepheids near the blue edge will therefore be affected, namely, only those that move redward and enter the IS. For the same reasons, there should also be a (50%) deficiency of Cepheids at the red edge. Furthermore, at a given period there will be a medley of Cepheids spread over the whole IS. Consequently, there should be an overall deficiency of low-amplitude Cepheids at all periods.

For RR Lyrae stars, we deduce from Dorman (1992) that  $dT_{\text{eff}}/dt \sim 1.2 \times 10^{-12} \text{ s}^{-1}$  when entering the overtone blue edge. From our linear models, we obtain  $d\kappa/dT_{\text{eff}} \sim 1.5 \times 10^{-9} (\text{K s})^{-1}$ , which leads to  $\chi \sim 1.8 \times 10^{-21} \text{ s}^{-2}$ . In the IS,  $\kappa_{\text{max}}$  is  $71 \times 10^{-9} \text{ s}^{-1}$ . We thus estimate that  $\hat{A}/A_{\text{max}} \sim 0.01$  at the blue edge and that the pulsation amplitude stays negligibly small for  $\hat{t} \sim 5000 \text{ yr}$ .

### 3.2. Switching to and from Double-Mode Pulsation

The coefficients of the amplitude equations (7a) and (7b) can be extracted from hydrodynamical simulations, as we illustrate for a sequence of RR Lyrae models. First, we compute the stable pulsational states at selected values in the  $T_{\text{eff}}$  range of interest. From these we extract for each model (characterized by  $T_{\text{eff}}$ ) the coefficients  $\kappa_0(T_{\text{eff}})$ ,  $q_{00}(T_{\text{eff}})$ , etc. The values of  $d \ln T_{\text{eff}}/dt$  along the evolutionary track through the IS determine the time dependence of  $\kappa_0(t)$ ,  $q_{00}(t)$ , etc.

We illustrate the method for an RR Lyrae star as it evolves through the switching from SM overtone to DM to SM fundamental pulsation. Figure 2 shows the results of



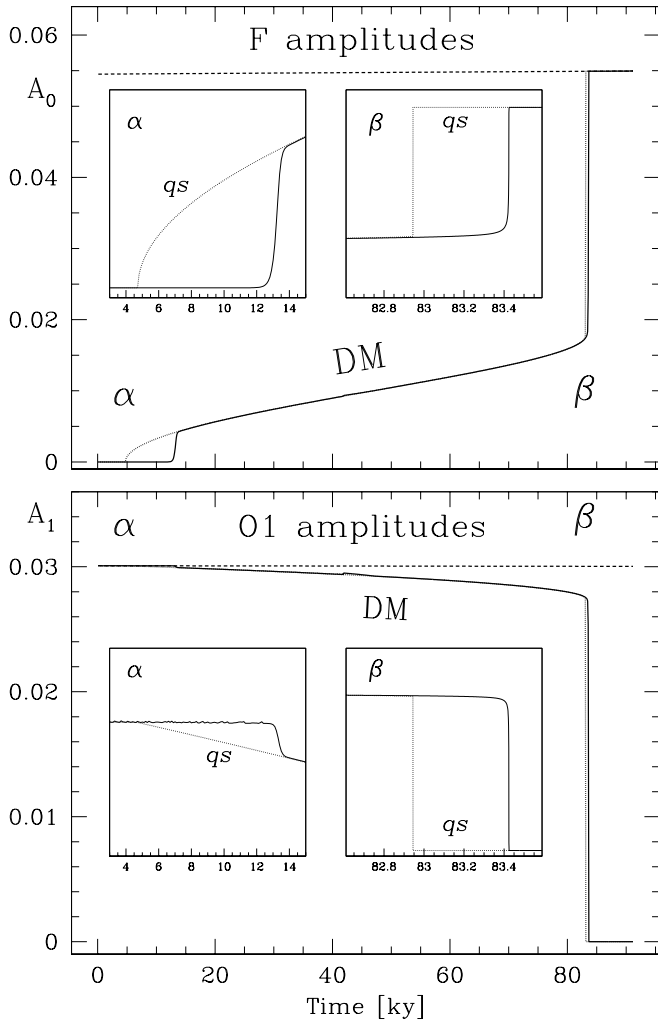


FIG. 2.—Redward evolution of the RR Lyrae model through the HR diagram. *Top*: Fundamental (F) SM amplitude or component amplitude in the DM. *Bottom*: O1 SM amplitude or component amplitude. Here  $\alpha$  marks switching from SM O1 to DM pulsation, and  $\beta$  switching from DM to the F limit cycle.

the integration of equations (7a) and (7b), i.e., the pulsation amplitudes of the F and O1 modes. For convenience, we have chosen a track with fixed luminosity  $L = 50 L_{\odot}$  and mass  $M = 0.77 M_{\odot}$ ,  $Z = 0.0001$ , rather than an inclined evolutionary track (Dorman 1992). The star is assumed to be evolving toward colder  $T_{\text{eff}}$ . The origin of time is arbitrarily taken to be a few thousand years before the point (marked  $\alpha$ ) where the O1 limit cycle becomes unstable to a DM pulsation (point  $\beta$ ).

Figure 2 is best understood in conjunction with paper KBSC02. (Their Fig. 3 shows the location of the SM and DM fixed points and their stability in an amplitude-amplitude plot for selected  $T_{\text{eff}}$ , while their Fig. 2 shows the variation of the quasi-static amplitudes along the sequence.) The solid lines here denote the pulsation amplitudes, or the component amplitudes in the case of DM pulsations, as a function of time; top graph for the F amplitude and bottom for the O1 amplitude. The dotted lines denote the quasi-static amplitudes, i.e., the instantaneous fixed points of equations (7a) and (7b).

### 3.2.1. Soft Bifurcation

The first inset in Figure 2 is a blowup of the onset of DM behavior near point ( $\alpha$ ). As expected, the behavior of the nascent F amplitude is very similar to the solution of equation (1) that was shown in Figure 1. The major difference is that here  $\chi$  becomes the rate of change of the linear stability coefficient of an F-mode perturbation of the O1 limit cycle (the Floquet stability exponent) rather than that of the linear growth rate of the mode.

One sees that, for DM onset as well, stellar evolution inhibits the growth of the pulsation amplitude for some 8000 yr, i.e., much beyond the thermal timescale, which is of the order of a hundred pulsations. DM RR Lyrae (RRd) with small fundamental mode component pulsation amplitudes should be rare.

### 3.2.2. Hard Bifurcation

An example of a hard bifurcation occurs in the second bifurcation for our RR Lyrae model, marked  $\beta$  in Figure 2. The stable DM is annihilated by a second unstable DM, and they both disappear (cf. Figs. 2 and 3 of KBSC02). In this case, the star gets attracted by the F fixed point, and thus the pulsation switches to a stable F limit cycle.

Figure 3 depicts the nature of the two RR Lyrae stellar models of Figure 1, taken on either side of point  $\beta$ , just before (*top panel*) and after (*bottom panel*) the DM fixed point vanishes. In this amplitude-amplitude diagram, the large filled circles represent the stable fixed points, of which now only the F fixed point is left in the bottom figure with amplitude  $A_0 = 0.055$ . The large open circle refers to the unstable O1 fixed point at  $A_1 = 0.030$ . The large square denotes the location of the just vanished pair of DMs.

The “velocity” flow field in the  $A_0$ - $A_1$  plane is given by  $\mathbf{u} = (\dot{A}_0, \dot{A}_1)$  and the speed by  $u = (\dot{A}_0^2 + \dot{A}_1^2)^{1/2}$ . The “arrows” in Figure 3 represent the normalized “velocity” flow field, i.e., the vectors  $\mathbf{u}/u$ . The dots denote the bases of the vectors. The gray scale indicates the log of the speed (length of the velocity vectors). Note that the typical “thermal” timescale is given by the shading near the origin.

It is very apparent that all the trajectories get attracted very rapidly to an arc going from the  $A_1$  axis to the  $A_0$  axis. This arc is an integral curve of the steady-state amplitude equations (known as a heteroclinic connection because it connects two different fixed points, viz., the O and F fixed points). Along this arc, the motion is considerably slower than thermal. The transition occurs on a timescale of  $\sim 100$  yr, very long compared to the thermal timescale of  $\kappa^{-1} \sim 100$  days.

At the moment the DM disappears, the star finds itself at the point marked with a large square (*bottom graph*), and it slowly gets attracted to the only stable fixed point, namely, F. The pulsation slowly changes from DM to fundamental SM.

In the case of a hard bifurcation, the switching time, even though of the “same order of magnitude” as the thermal timescale, thus can exceed it by factors of 10.

### 3.2.3. Speed along Heteroclinic Connection

Finally, we examine why the speed is slow along the heteroclinic connections that link the SM and the DM fixed points. In Figure 3, one visualizes the location of these heteroclinic connections from the vector field. (They are shown explicitly in Fig. 1 of KBSC02.) Consider now the two loci

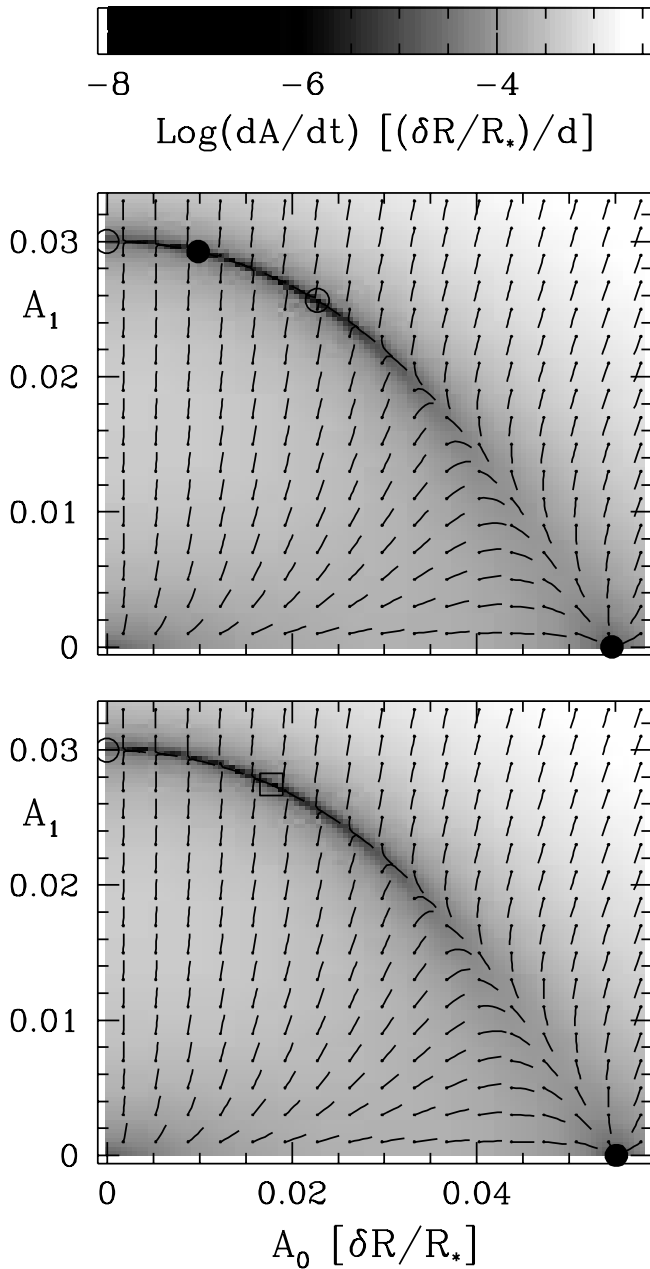


FIG. 3.—F amplitude–O1 amplitude phase space for two RR Lyrae models with a 10 K difference in effective temperature, where the top one has the higher temperature. The short lines represent the normalized flow field (with the dots representing the bottom of the vectors). The large filled/open circles in the top graph denote the location of the stable/unstable fixed points. The square in the bottom graph denotes the location of the just vanished pair of DMs. The speed of the flow is represented by the gray scale. The amplitudes refer to  $(\delta R/R)_{\text{surf}}$ .

that are defined by setting the first and second of equations (7a) and (7b) equal to zero, respectively. On these loci, either the horizontal ( $A_1$ ) or the vertical ( $A_2$ ) speed vanishes by definition. These loci each emanate from one of the two SM fixed points, and both of them intersect the heteroclinic connection at the two DM points. The heteroclinic connection lies, therefore, very close to the two loci, especially near and in between the DM fixed points, and the speed  $u = [(A_1)^2 + (A_2)^2]^{1/2}$  must therefore also remain small.

One also notes that, when both modes are linearly unstable, which is the situation we are interested in, the heteroclinic connection is always attractive sideways. This remains true a fortiori when the loci intersect and give rise to a DM fixed point (in which case the speed vanishes at the DM).

Note also that the linear stability root of the F fixed point along the  $A_0$  axis is given by  $-2\kappa_0$ , and since  $\kappa_0$  is typically large, the speed along  $A_0$  is high. Mutatis mutandis, one shows that the speed along the  $A_1$  axis is also high. Although this only concerns the motion along the coordinate axis, Figure 3 shows that it remains true in between.

#### 4. CONCLUSION

We have shown that there are two types of bifurcations with different characteristics. The first is a soft bifurcation in which the incipient mode starts with infinitesimal amplitude, whose growth is determined by the evolutionary rate of change  $\chi = d\kappa/dt$  of the appropriate linear growth rate  $\kappa$ . This timescale  $\chi^{-1/2}$  can be very large compared to the thermal timescale  $\kappa^{-1}$ , depending on the stellar evolution timescale. The second is a hard bifurcation that occurs when the rug is pulled out from under the pulsation, as it were, i.e., when the pulsation must change because, as a result of an evolutionary change in the star's structure, it is no longer allowed or possible. Here the timescale remains thermal, but generally with a large multiplication factor. One consequence of this delay and then abrupt onset of pulsation is that stellar pulsators with low amplitudes should be rarely observed, in agreement with observations.

Another interest of this paper is that it shows the possibility of obtaining valuable information about stellar structure from the observations of a star that is in the process of starting to pulsate or of switching its pulsational state. In a subsequent paper, we will show how the combined use of numerical hydrodynamics, time-series analysis, the amplitude equation formalism, and the knowledge of the stellar evolution timescale ( $dT_{\text{eff}}/dt$ ) allow one to consistently compute the evolution of a pulsating star throughout the whole IS.

This work has been supported by NSF grant AST 98-19608 and by the Hungarian Scientific Research Fund (OTKA; T-038440). We also wish to thank an anonymous referee for his suggestions.

#### REFERENCES

- Alibert, Y., Baraffe, I., Hauschildt, P., & Allard, F. 1999, *A&A*, 344, 551
- Bergé, P., Pomeau, Y., & Vidal, C. 1986, *Order Within Chaos* (New York: Wiley)
- Bono, G., Castellani, V., & Stellingwerf, R. F. 1995, *ApJ*, 445, L145
- Bono, G., Marconi, M., & Stellingwerf, R. F. 2000, *A&A*, 360, 245
- Buchler, J. R. 1993, in *Nonlinear Phenomena in Stellar Variability*, ed. M. Takeuti & J. R. Buchler (Dordrecht: Kluwer), 9
- Buchler, J. R. 1998, in *ASP Conf. Ser. 135, A Half Century of Stellar Pulsation Interpretations*, ed. P. A. Bradley & J. A. Guzik (San Francisco: ASP), 220
- Buchler, J. R., & Goupil, M. J. 1984, *ApJ*, 279, 394
- Buchler, J. R., & Kovács, G. 1987, *ApJ*, 318, 232
- Clement, C. M., & Goranskij, V. P. 1999, *ApJ*, 513, 767
- Coulet, P., & Spiegel, E. A. 1984, *SIAM J. Appl. Math.*, 43, 776

- Dorman, B. 1992, *ApJS*, 81, 221  
Ferne, D. J., Beattie, B., Evans, N. R., & Seager, S. 1996, *IBVS* No. 4148  
Feuchtinger, M. U. 1998, *A&A*, 337, L29  
———. 1999, *A&A*, 351, 103  
Feuchtinger, M., Buchler, J. R., & Kolláth, Z. 2000, *ApJ*, 544, 1056  
Kamper, K. W., & Fernie, J. D. 1998, *AJ*, 116, 936  
Kolláth, Z., Beaulieu, J. P., Buchler, J. R., & Yeecko, P. 1998, *ApJ*, 502, L55  
Kolláth, Z., & Buchler, J. R. 2001, Double-Mode Stellar Pulsations, in *Nonlinear Studies of Stellar Pulsation*, ed. M. Takeuti & D. D. Sasselov (Dordrecht: Kluwer), 29 (KB01)  
Kolláth, Z., Buchler, J. R., & Feuchtinger, M. 2000, *ApJ*, 540, 468  
Kolláth, Z., Buchler, J. R., Szabó, R., & Csubry, Z. 2002, *A&A*, 385, 932 (KBSC02)  
Lebovitz, N. 1990, in *Ann. NY Acad. Sci.*, 617, 73  
Moskalik, P., Buchler, J. R., & Marom, M. 1992, *ApJ*, 385, 685  
Stellingwerf, R. F. 1975, *ApJ*, 195, 441  
Udalski, et al. 1997, *Acta Astron.*, 47, 1  
———. 1999, *Acta Astron.*, 49, 1  
Walker, A. 1998, *AJ*, 116, 220  
Walker, A., & Nemec, J. M. 1996, *AJ*, 112, 2026